Phase Relation, Crystal Structures, and Magnetic Properties of Nd−Co−B Borides

Yi. Chen,*,† X. Li,‡ X. L. Chen,† J. K. Liang,† G. H. Rao,† B. G. Shen,† Q. L. Liu,† L. P. Jin,‡ and M. Z. Wang‡

Institute of Physics and Center for Condensed Matter Physics, Chinese Academy of Sciences, Beijing 100080, People's Republic of China, and Department of Chemistry, Beijing Normal University, Beijing, 100875, People's Republic of China

Received July 22, 1999. Revised Manuscript Received February 3, 2000

The phase relation of the ternary system Nd−Co−B quenched from 600 °C in the Co-rich region has been determined by means of X-ray powder diffraction. In this region there exist 11 ternary borides: $Nd_3Co_{13}B_2$, $NdCo_4B$, $Nd_5Co_{19}B_6$, $Nd_3Co_{11}B_4$, $Nd_2Co_7B_3$, $Nd_2Co_{14}B$, $NdCo_{12}B_6$, $NdCo_4B_4$, $Nd_2Co_5B_3$, $NdCo_2B_2$, and $Nd_2Co_5B_2$. The first five borides are members of the homologous series $Nd_{m+n}Co_{5m+3n}B_{2n}$ (or $NdCo_{5-x}B_x$). New layered borides $Nd_3Co_{13}B_2$ and $Nd_5Co_{19}B_6$ have not been reported previously. The space group of them is $P6/mmm$ and their crystal structures are refined by the Rietvled method. All the compounds of this $Nd_{m+n}Co_{5m+3n}B_{2n}$ family magnetically order between $T_C = 710$ K for $Nd_3Co_{13}B_2$ and $T_C = 330$ K for $Nd_2Co_7B_3$. The mean cobalt moments of the $Nd_{m+n}Co_{5m+3n}B_{2n}$ borides determined at 4.2 K are strongly dependent on the composition. On the basis of the experimental results, three kinds of Co sites with different magnetic moments are proposed. It is shown that increasing B content in $NdCo_{5-x}B_x$ borides leads to an increase of the second-order crystal-field parameters A_{20}, which explains the enhancement of the magnetocrystalline anisotropy. Spin reorientations are observed in $Nd_3Co_{13}B_2$ and $Nd_3Co_{11}B_4$ compounds. The magnetic phase diagram of the $Nd_{m+n}Co_{5m+3n}B_{2n}$ borides is also given, and the behavior of magnetocrystalline anisotropy is analyzed using the single ion model.

Introduction

Since the discovery of the excellent permanent magnetic materials $Nd_2Fe_{14}B$,[1] a worldwide search for other magnetic materials has been carried out. It is believed that there exist many other novel compounds in the still unexploited reservoir of ternary compounds containing rare earth (R) and transition metals (T).[2] Out of approximately 100 000 possible ternary compounds, phase diagram information is available on fewer than 6000 of them.[3] Often, this information is far from complete, relating to only a single isothermal section or a limited composition field. The emergence of $R(FeM)_{12}A_\delta$ (M = Ti, V, Cr, Mo, Mn, Nb, etc. and A = H, C, N)[4] compounds with $ThMn_{12}$-type structure and $R_2Fe_{17}A_\delta$[5] compounds with Th_2Zn_{17}- or Th_2Ni_{17}-type structure as promising candidates for permanent magnets encourages the further exploitation of magnetic materials in R−T−M systems.[6−7] In these iron-rich 1:12 and 2:17 structures, the interstitial modification with light elements such as carbon or nitrogen to the interstitial sites has been found to be a very effective way to improve the magnetic properties.[8−10] As a typical materials, $Sm_2Fe_{17}(C_{1-x}N_x)_{3-\delta}$ has a Curie temperature T_C of 758 K (T_C = 588 K for $Nd_2Fe_{14}B$), a saturation magnetization ($\mu_0 M_S$) of 1.5 T at room temperature, and an anisotropy field ($\mu_0 H_a$) of 15 T, making it the most promising compound for permanent magnet application since the discovery of $Nd_2Fe_{14}B$.[11]

Recently, a series of ternary intermetallic compounds, $R_3(FeM)_{29}$,[12] located at the iron-rich corner of the R−Fe phase diagrams and stabilized by a third element M, was discovered. The structure of $R_3(FeM)_{29}$ compounds can be considered as an intermediate structure between the well-known 2:17 and 1:12 structures consisting of a combination of the 2:17 and 1:12 units in a ratio of 1:1. All of them are derived by different means of dumbbell 2(Fe,M) substitution for R in the $CaCu_5$-type structure.

† Chinese Academy of Sciences.
‡ Beijing Normal University.

(1) Sagawa, M.; Fujimura, S.; Togawa, M.; Matsuura, Y. *J. Appl. Phys.* **1984**, *55*, 2083.
(2) Buschow, K. H. J. *Pep. Prog. Phys.* **1991**, *54*, 1123.
(3) Li, H. S.; Coey, J. M. D. *Handbook of MagneticMaterials*; Buschow, K. H. J., Ed.; Elsevier Science Publishers B.V.: New York, 1991; p 6.
(4) Yang, Y. C.; Zhang, X. D.; Ge, S. L.; Pan, Q.; Ding, Y. F. *Proceeding of the Sixth International Symposium on Magnetic Anisotropy and Coercivity in Rare-Earth-Transition-Metal Alloys*; Carnegie Mellon University Press: Pittsburgh, PA, 1990; p 191.
(5) Coey, J. M. D.; Sun, H. *J. Magn. Magn. Mater.* **1990**, *87*, L251.
(6) Buschow, K. H. J. In *Ferromagnetic Materials, A Handbook on the Properties of Magnetically Ordered Substances*; (edited by E. P. Wohlfarth, E. P., Ed.; North-Holland: Amsterdam, 1988; p 4.
(7) Szytula, A.; Leciejiewica, J. *Handbook of Crystal Structure and Magnetic properties of Rare-earth Intermetalics*; CRC Press: Boca Raton, FL, 1994.
(8) Yang, Y. C.; Zhang, X. D.; Ge, S. L.; Pan, Q. Ding, Y. F. *Appl. Phys. Lett.* **1991**, *58*, 2042.
(9) Sun, H.; Otani, Y.; Coey, J. M. D. *J. Appl. Phys.* **1990**, *67*, 4659.
(10) Katter, M.; Wecker, J.; Schultz, L. *J. Magn. Magn. Mater.* **1990**, *92*, L14.
(11) Qi, Q. N.; Sun, H.; Skomski, R.; Coey, J. M. D. *Phys. Rev. B* **1992**, *45*, 12278.
(12) Ivanova, G. V.; Shcherbakova, Y. V.; Belozerov, Y. V.; Yermolenko, A. S. Y.; Teyel, I. *Phys. Met. Metallogr.* **1990**, *70*, 63.

10.1021/cm990462f CCC: $19.00 © 2000 American Chemical Society
Published on Web 04/14/2000

Like 2:17 and 1:12 compounds, the compounds $R_3(FeM)_{29}$ are able to absorb N or C as interstitial atoms, leading to a remarkable improvement in their magnetic properties.[13] The Curie temperature is enhanced to ~700 K in $R_3(FeM)_{29}A_\delta$, which is comparable to that of $R_2Fe_{17}N_\delta$. The room-temperature saturation magnetization, $\mu_0 M_S \sim 1.5$ T, is also close to that of $R_2Fe_{17}N_\delta$. Significant coercivity has been developed, reaching 0.8 T in $Sm_3(Fe_{1-x}M_x)_{29}N_\delta$. These promising magnetic properties suggest that the $Sm_3(Fe_{1-x}M_x)_{29}N_\delta$ compounds might be alternative nitride hard magnets.[14]

However, these nitrides and carbides prepared by the gas-phase reaction have a major drawback, namely their chemical or structure instability at high temperatures. They will completely decompose into α-Fe and RN or RC at about 600−700 °C. The poor thermal stability restricts their practical application as a sintered magnet. Therefore, it is important to search for the alternative hard magnets to these nitrides and carbides. It was found that there exist some Co-rich phases in the R−Co−B systems.[15] For example, a homologous series of compounds exists between the compositions RCo_5 and RCo_3B_2.[16] This series can be represented by a general formula $R_{1+n}Co_{5+3n}B_{2n}$, which is formed by alternating stacking of one layer RCo_5 and *n* layers RCo_3B_2 along the *c* axis. Huge magnetic anisotropy has been found in the $Sm_{1+n}Co_{5+3n}B_{2n}$ system: the anisotropy fields of $SmCo_5$, $SmCo_4B$, $Sm_3Co_{11}B_4$, and $SmCo_3B_2$ are found to be 71, 120, 116, and 130 T at 4.2 K, respectively.[17] However, the Curie temperature (T_C < 500 K) and saturation moment of these $R_{1+n}Co_{5+3n}B_{2n}$ intermetallics are too low to be suitable for permanent magnet fabrication.[18−22] To overcome these drawbacks, many investigations have been focused on either substituting Co by Fe or preparing materials with interstitial atom modifications by gas−solid reactions.[23−24] Here, we show an alternative strategy, in which we propose a similar series $R_{m+n}Co_{5m+3n}B_{2n}$ with higher Co contents. This series, crystallographically analogous to $R_{1+n}Co_{5+3n}B_{2n}$, is expected to consist of m layers RCo_5 and *n* layers RCo_3B_2. After we carefully investigated the phase diagrams of R−Co−B (R = Pr, Nd, Sm, Gd) systems at relatively low temperatures, two new series of high Co compounds $R_3Co_{13}B_2$ and $R_5Co_{19}B_6$ were confirmed to exist.[25−27] The fact that all the compounds of $R_3Co_{13}B_2$ have high Curie temperatures(≥700K) and exhibit large anisotropy fields makes them very promising candidates for permanent magnets. In addition, the $R_{m+n}Co_{5m+3n}B_{2n}$ intermetallics provide a very good opportunity to investigate the exchange interactions and anisotropies of the 3d and 4f sublattice because the magnetic properties are expected to reflect the crystal structure changes depending on different *m* and *n*. In this paper, we present a more complete study on crystal structures and magnetic properties of the $Nd_{m+n}Co_{5m+3n}B_{2n}$ intermetallics. Furthermore, the phase relation of Nd−Co−B system is also reported, which is significant for the fundamental research and practical application of the materials.

Experimental Section

The samples examined in this work were prepared by melting raw materials of more than 99.9% purity in an arc furnace. To avoid the loss of boron during melting, boron was added through a master alloy of CoB. To ensure the homogeneity of the samples, the ingots were turned and melted several times. The weight loss of the samples during melting was less than 1%. After arc melting, the samples were wrapped in Ta foil and sealed in a quartz tube. The samples were annealed in a vacuum at 873 K for 2 months and then rapidly cooled to room temperature. The phase identification of the samples was carried out by X-ray powder diffraction, using a four-layer monochromatic focusing Guinier de Wolff camera with Co Kα radiation. The X-ray diffraction (XRD) data, used to determine the crystal structure parameters, were obtained in a Rigaku Rint diffractometer with Cu Kα radiation with graphite monochromator, operating in a step-scan mode with a scanning step of $2\theta = 0.02°$ and a sampling time of 2s. The XRD pattern of a sample consisting of powder particles (≤40 μm), which were magnetically aligned at room temperature, was used to determine the easy magnetization direction (EMD) in these compounds. For the investigated compound with the EMD in the basal plane at room temperature, the magnetic alignment was carried out by means of the rotation−alignment technique, while the sample, which has uniaxial anisotropy at room temperature, was static−magnetically aligned. The magnetic isothermal curves were measured at 5 K in a SQUID in a magnetic field ranging from 0 to 65 kOe.

Results and Discussion

The 42 ternary alloys were prepared in the Co-rich region of Nd−Co−B ternary system and annealed at 873 K for three months. Phase identification of these samples was carried out by X-ray powder diffraction. Eleven ternary compounds were observed on the Co-rich side of Nd−Co−B system: $Nd_3Co_{13}B_2$ (1), $NdCo_4B$ (2), $Nd_5Co_{19}B_6$ (3), $Nd_3Co_{11}B_4$ (4), $Nd_2Co_7B_3$ (5), $Nd_2Co_{14}B$ (6), $NdCo_{12}B_6$ (7), $NdCo_4B_4$ (8), $Nd_2Co_5B_3$ (9), $NdCo_2B_2$ (10), and $Nd_2Co_5B_2$ (11). Eight of them were reported in the paper of Kuz'ma.[21] We found that $Nd_2Co_{14}B$ with the tetragonal $Nd_2Fe_{14}B$-type structure still exists in our ternary alloys quenched from 600 °C. The layered borides $Nd_3Co_{13}B_2$ and $Nd_5Co_{19}B_6$ have not been reported previously. They belong to the homologous series $R_{m+n}Co_{5m+3n}B_{2n}$ which were described in our previous papers.[25−27] $Nd_2Co_5B_2$ is a member of the homologous series $R_{m+n}Co_{2m+3n}B_{2n}$ which is based on the $MgZn_2$ type and $CeCo_3B_2$-type structures. On the basis

(13) Yang, F. M.; Nasunjilegal, B.; Wang, J. L.; Zhu, J. J.; Qin, W. D.; Tang, N, Zhao, R. W.; Hu, B. P.; Wang,; Y. Z.; Li, H. S. *J. Phys.: Condes. Matter* **1995**, *7*, 1679.
(14) Suzuki, S.; Suzuki, S.; Kawasaki, M. *IEEE Trans. Magn.* **1995**, *31*, 3695.
(15) Stadelmaier, H. H.; Hyung, J. L. *Z. Metallkde.* **1978**, *69*, H.11.
(16) Kuz'ma, Yu. B.; Chernyak, G. V. *J. Less-Commom. Metal.* **1983**, *90*, 217.
(17) Ido, H.; Sugiyama, K.; Hachino, H.; Date, M.; Cheng, S. F.; Maki, K. *Physica B* **1992**, *177*, 265.
(18) Streever, R. L. *Phys. Rev. B* **1979**, *19*, 2704.
(19) Tasset, F. Ph.D. Thesis, University of Grenoble, 1975.
(20) Smit, H. H.; Thiel, R. C.; K. Buschow, H. J. *J. Phys. F: Met. Phys.* **1988**, *18*, 295.
(21) Pedziwatr, A. T.; Jiang, S. Y.; Wallace, W. E.; Burzo, E.; Pop, V. *J. Magn. Magn. Mater.* **1987**, *66*, 69.
(22) Tetean, R.; Burzo, E. *J. Magn. Magn. Mater.* **1996**, *157/158*, 633.
(23) Nadia, A. E.; Stadelmaier, H. H. *Z. Metallkde.* **1983**, *74* H.2, 86.
(24) Huang, M. Q.; Ma, B. M.; L. Zhang, Y.; Wallace, W. E.; Sankar, S. G. *J. Appl. Phys.* **1990**, *67*, 4981.
(25) Chen, Y.; Liu, Q. L.; Liang, J. K.; Chen, X. L.; Shen, B. G. *Appl. Phys. Lett.* **1999**, *74* (6), 856.
(26) Chen, Y.; Chen, X. L.; Liang, J. K.; Shen, B. G.; Liu, Q. L. *J. Phys.: Condens. Matter.* **1999**, *11* (42) 8251.
(27) Chen, Y.; Liang, J. K.; Liu, Q. L.; Chen, X. L. *J. Alloys Compd.* **1999**, *288*, 170.

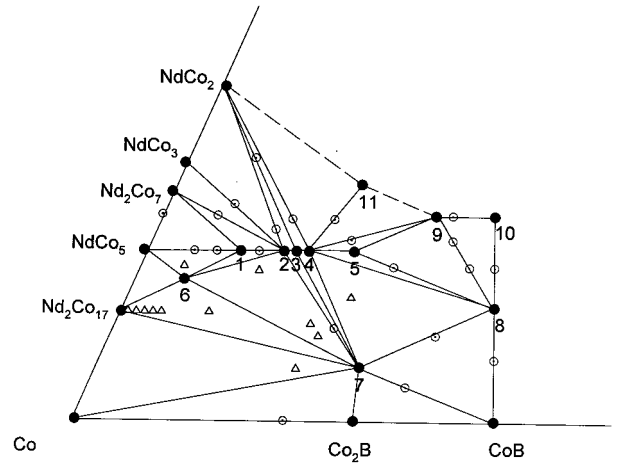

Figure 1. Isothermal section for the ternary system Nd−Co−B quenched from 600 °C. Filled cycles are single phases, dotted cycles two phases, and diamonds three phases: 1, $Nd_3Co_{13}B_2$; 2, $NdCo_4B$; 3, $Nd_5Co_{19}B_6$; 4, $Nd_3Co_{11}B_4$; 5, $Nd_2Co_7B_3$; 6, $Nd_2Co_{14}B$; 7, $NdCo_{12}B_6$; 8, $NdCo_4B_4$; 9, $Nd_2Co_5B_3$; 10, $NdCo_2B_2$; 11, $Nd_2Co_5B_2$.

Table 1. Ternary Nd−Co−B Borides

compounds	structure type	space group	lattice parameters		
			a (Å)	*b* (Å)	*c* (Å)
(1) $Nd_3Co_{13}B_2$	$La_3Ni_{13}B_2$	*P*6/*mmm*	5.072		10.784
(2) $NdCo_4B$	$CeCo_4B$	*P*6/*mmm*	5.086		6.901
(3) $Nd_5Co_{19}B_6$	$Lu_5Ni_{19}B_6$	*P*6/*mmm*	5.133		16.652
(4) $Nd_3Co_{11}B_4$	$Ce_3Co_{11}B_4$	*P*6/*mmm*	5.140		9.742
(5) $Nd_2Co_7B_3$	$Ce_2Co_7B_3$	*P*6/*mmm*	5.159		12.767
(6) $Nd_2Co_{14}B$	$Nd_2Fe_{14}B$	$I4_2/mnm$	8.646		11.865
(7) $NdCo_{12}B_6$	$SrNi_{12}B_6$	*R*3*m*	9.502		7.471
(8) $NdCo_4B_4$	$NdCo_4B_4$	$P4_2/n$	7.070		3.822
(9) $Nd_2Co_5B_3$	−	*Ccca*	5.13	38.2	10.77
(10) $NdCo_2B_2$	$BaAl_4$	*I*4/*mmm*	3.586		9.747
(11) $Nd_2Co_5B_2$	$Ce_2Co_5B_2$	$P6_3/mmc$	5.115		20.565

of the experimental results, the isothermal section of the ternary system is constructed (Figure 1). The 11 compounds are identified with points numbered 1 to 11. All triangular fields in Figure 1 represent three-phase regions. No solid solution was detected by the measurement of the lattice parameters for all phases. The crystal structure data of the ternary compounds are summarized in Table 1.

The borides $NdCo_5$, $Nd_3Co_{13}B_2$, $NdCo_4B$, $Nd_5Co_{19}B_6$, $Nd_3Co_{11}B_4$, and $Nd_2Co_7B_3$ belong to the homologous series $R_{m+n}Co_{5m+3n}B_{2n}$ (or $RCo_{5-x}B_x$), which is formed by alternating stacking of *m* layers RCo_5 and *n* layers RCo_3B_2 along the *c* axis (Figure 2a−f). They correspond to the values of $m = \infty$ and $n = 1$, $m = 2$ and $n = 1$, $m = 1$ and $n = 1$, $m = 2$ and $n = 3$, $m = 1$ and $n = 2$, $m = 1$ and $n = 3$, respectively. $NdCo_3B_2$ does not exist in our phase diagram. It can be seen in Table 1 that the change in lattice parameters of these borides follows basically the relation: $a \approx a_{RCo_5}$, $c \approx mc_{RCo_5} + nc_{RCo_3B_2}$. Among these borides, the $R_3Co_{13}B_2$ and $R_5Co_{19}B_6$ are of particular interest.[26−27] We found that they are formed by peritectoid reaction and exist only at relatively low temperatures below 1073 K. The possible reactions involve $NdCo_5 + 2NdCo_4B \leftrightarrow Nd_3Co_{13}B_2$ for $Nd_3Co_{13}B_2$ and $2NdCo_4B + Nd_3Co_{11}B_4 \leftrightarrow Nd_5Co_{19}B_6$ for $Nd_5Co_{19}B_6$, respectively. To obtain pure phases, it generally needs prolonged annealing of several months at relatively low temperatures. Figure 3a shows the X-ray powder diffraction pattern of $Nd_3Co_{13}B_2$ annealed at 873 K for three months. The XRD patterns can be successfully indexed with a hexagonal cell with lattice parameters $a = 5.0722(4)$ Å and $c = 10.7840(5)$ Å.[28] The space group is *P*6/*mmm*. An initial structure model was derived from the isostructural $La_3Ni_{13}B_2$ compound and then refined by using the program DBW-9411.[29] The Rietveld refinement results are shown in Figure 3a and Table 2. The pattern factor R_p, the weighted pattern factor R_w, and the expected pattern factor R_{exp} are 12.5%, 17.1%, and 6.7%, respectively. There is one $Nd_3Co_{13}B_2$ formula unit in the cell: Nd atoms are distributed in two different crystallographic sites (1a, 2e), the Co atoms in three different positions (4h, 6i, 6i, 3g), and boron is located in 2c position. The crystal structure of $Nd_3Co_{13}B_2$ is illustrated in Figure 2b. Figure 3b shows the XRD pattern for $Nd_5Co_{19}B_6$ annealed at 873 K for three months. It can be successfully indexed with a hexagonal cell with lattice parameters $a = 5.1328(3)$ Å and $c = 16.6519(5)$ Å. An initial structure model was derived from the isostructural $Lu_5Ni_{19}B_6$ based on the space group *P*6/*mmm*. There is one $Nd_5Co_{19}B_6$ formula unit in the cell: the Nd atoms occupy three different crystallographic sites (1b, $2e_1$, $2e_2$), the Co atoms four different positions ($4h_1$, $6i_1$, $6i_2$, 3f) and B the 2d and $4h_2$ positions. Rietveld refinement[29] was performed and the final refinement results are shown in Figure 3b and Table 3. The pattern factor R_p, the weighted pattern factor R_w, and the expected pattern factor R_{exp} are 13.6%, 17.3%, and 6.9%, respectively. The crystal structure of $Nd_5Co_{19}B_6$ is illustrated in Figure 2d.

Figure 4 shows the temperature dependence of the magnetization, $M(T)$, for the free powder samples of $Nd_{m+n}Co_{5m+3n}B_{2n}$ in a low field of 0.05 T. The T_C is determined from $M^2 - T$ plots by extrapolating M^2 to zero. The B concentration dependence of the T_C is illustrated in Figure 5a. We found that the Curie temperature decreases monotonically as the B concentration increases. Generally, the Curie temperature of Nd−Co compounds is determined by the three different exchange-coupling constants: J_{CoCo}, J_{NdCo}, and J_{NdNd}. The Nd−Nd interaction is generally neglected because it is smaller than the Co−Co and Nd−Co interaction. The 3d−4f interaction J_{Nd-Co} has only a minor influence on the Curie temperature. However it dominates the molecular field experienced by the Nd moment that, in turn, determines the temperature dependence of the magnetic moment and the magnetocrystalline anisotropy of Nd ions. Since the Co−Co exchange coupling constants are 1 order of magnitude larger than the Nd−Co exchange coupling constants, the Curie temperature for two-sublattice Nd-T compounds is mainly determined by the Co−Co interaction. Thus, the T_C of $Nd_{m+n}Co_{5m+3n}B_{2n}$ can be written as

$$T_C = \{T_{NdNd} + T_{CoCo} + [(T_{NdNd} - T_{CoCo})^2 + 4T_{NdCo}]^{1/2}\}/2 \quad (1)$$

(28) Werner, P. E. *Z. Kristallogr.* **1964,** 120, 375; *J. Appl. Crystallogr.* **1976**, *9*, 216.
(29) Rietveld, H. M. *Acta Crystallogr.* **1967**, *229*, 151; *J. Appl. Crystallogr.* **1969**, *2*, 65. Young, R. Y.; Sakthirel, A.; Moss, T. S.; Paiva-Santos, C. O. *J. Appl. Crystallogr.* **1995**, *28*, 366.

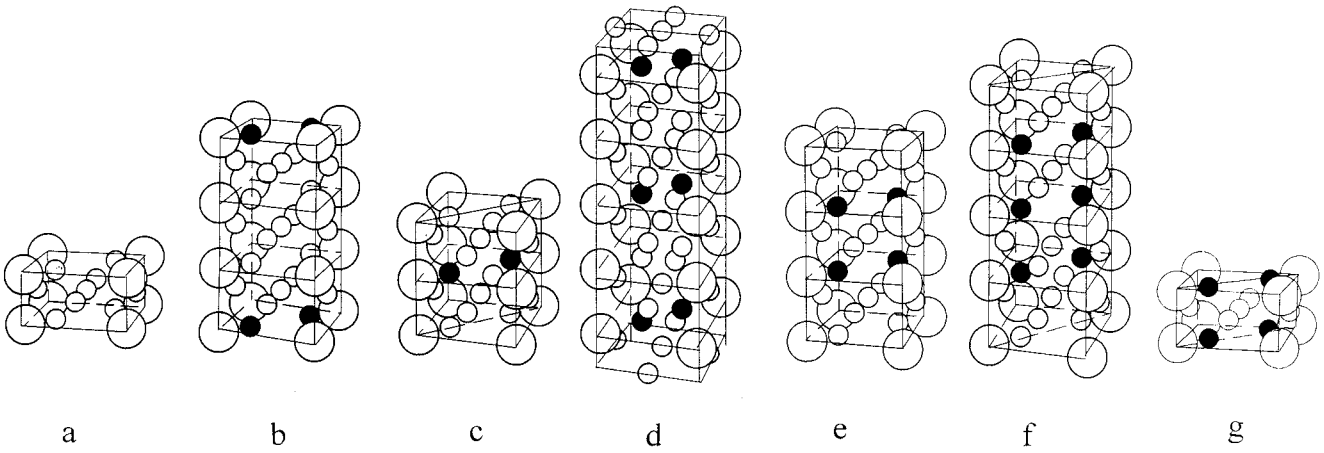

Figure 2. The crystal structures of $Nd_{m+n}Co_{5m+3n}B_{2n}$ borides. Large open circles are rare earth, small open circles cobalt, and filled ones boron: a, $NdCo_5$; b, $Nd_3Co_{13}B_2$; c, $NdCo_4B$; d, $Nd_5Co_{19}B_6$; e, $Nd_3Co_{11}B_4$; f, $Nd_2Co_7B_3$; g, $NdCo_3B_2$.

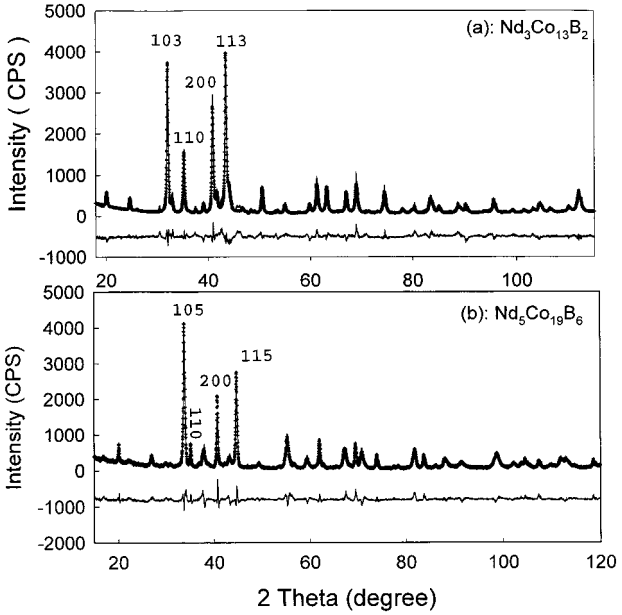

Figure 3. Output from Rietveld analysis of the XRD pattern of $Nd_3Co_{13}B_2$ (a) and $Nd_5Co_{19}B_6$ (b). The observed data are indicated by crosses and the calculated profile by the continuous line overlaying them. The lower curve is the difference between the observed and calculated intensity at each step.

Table 2. Atomic Positions and the Lattice Parameters of the $Nd_3Co_{13}B_2$. Space group: *P6/mmm*

atom	position	*x/a*	*y/b*	*z/c*
1Nd	1a	0	0	0
2Nd	2e	0	0	0.3292(4)
4Co	4h	0.3333	0.6667	0.3159(8)
6Co	6i	0.5000	0	0.1346(3)
3Co	3g	0.5000	0	0.5000
2B	2c	0.3333	0.6667	0

$z = 1$ $a = 5.0722$ Å $c = 10.7840$ Å
$R_p = 12.5\%$ $R_{wp} = 17.1\%$, $R_{exp} = 6.7\%$

Where contributive temperature T_{ii} (i = Nd, Co) and T_{NdCo} can be written as

$$T_{ii} = (2A_{ii}Z_{ii}G_i)/(3k_B) \quad (2)$$

and

$$T_{NdCo} = [2A_{NdCo}(Z_{NdCo}Z_{CoNd}G_{Nd}G_{Co})]^{1/2} \quad (3)$$

Table 3. Atomic Positions and the Lattice Parameters of the $Nd_5Co_{19}B_6$. Space Group: *P6/mmm*

atom	position	*x/a*	*y/b*	*z/c*
1Nd	1b	0	0	0.5000
2Nd	$2e_1$	0	0	0.0964(1)
2Nd	$2e_2$	0	0	0.2976(1)
4Co	$4h_1$	0.3333	0.6667	0.2955(2)
6Co	$6i_1$	0.5000	0	0.1742(1)
6Co	$6i_2$	0.5000	0	0.4114(1)
3Co	3f	0.5000	0	0
2B	2d	0.3333	0.6667	0.5000
4B	$4h_2$	0.3333	0.6667	0.0936(16)

$z = 1$ $a = 5.1328$ Å $c = 16.6519$ Å
$R_p = 13.6\%$ $R_{wp} = 17.3\%$ $R_{exp} = 6.9\%$

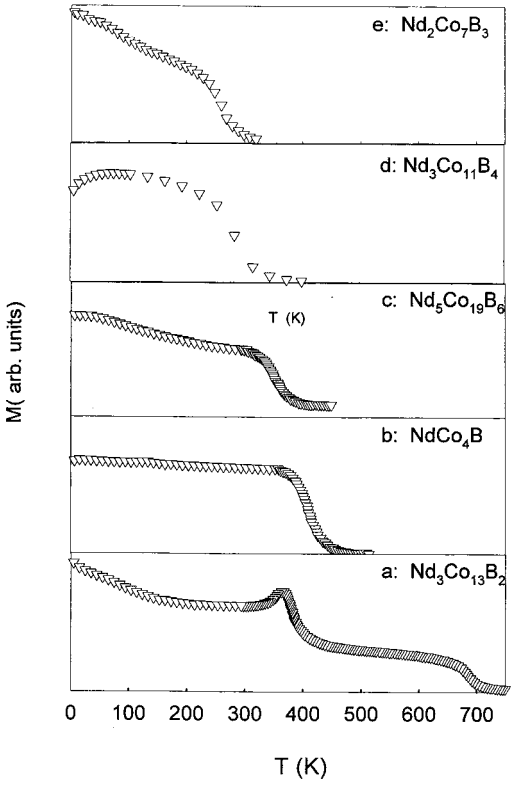

Figure 4. The temperature dependence of the magnetization, *M*(*T*), for the free powder samples of $Nd_{m+n}Co_{5m+3n}B_{2n}$ borides in a low field of 0.05 T.

where $G_i = (g_i - 1)^2 J_i(J_i + 1)$, Z_{ij} is the number of nearest j atom neighbor of an i atom, g_i is the Lande

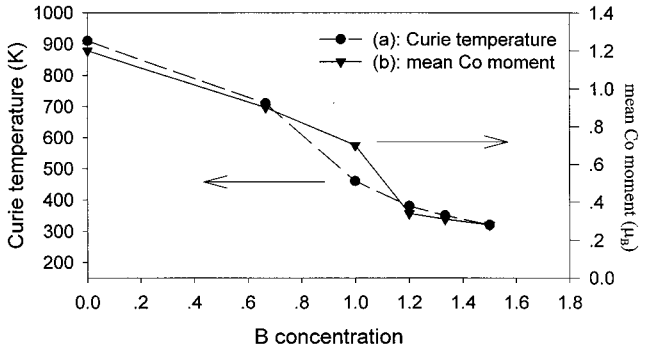

Figure 5. The B concentration dependence of T_C (filled cycles) and $\langle\mu_{Co}\rangle$ (filled triangles) of the $NdCo_{5-x}B_x$ borides. ($x = 0$, $NdCo_5$; $x = 0.67$, $Nd_3Co_{13}B_2$; $x = 1$, $NdCo_4B$; $x = 1.2$, $Nd_5Co_{19}B_6$; $x = 1.33$, $Nd_3Co_{11}B_4$; $x = 1.5$, $Nd_2Co_7B_3$).

Table 4. Curie Temperature (T_C), Spin Reorientation Temperature (T_{SR}), Saturation Magnetization (M_S) at 5 K, the Mean Co Moment ($\langle\mu_{Co}\rangle$), Anisotropy Field (H_A) at 5 K, and Easy Magnetization Direction (EMD) of $Nd_{m+n}Co_{5m+3n}B_{2n}$

compounds	T_c (K)	T_{SR} (K)	M_s (4.2K) (μ_B/f.u.)	$\langle\mu_{Co}\rangle$ (μ_B)	H_A(5 K) (kOe)	EMD (298 K)
$NdCo_5$	910		9.1	1.2	30	plane
$Nd_3Co_{13}B_2$	710	370	20.8	0.9	180	plane
$NdCo_4B$	460		5.8	0.7	100	axial
$Nd_5Co_{19}B_6$	380		21.5	0.34	340	plane
$Nd_3Co_{11}B_4$	350	100	12.4	0.31	490	plane
$Nd_2Co_7B_3$	320		8.0	0.28		plane

factor of the i atom, and A_{ii} and A_{NdCo} are averaged exchanged constants corresponding to Z_{ij}, respectively. The fact that the Curie temperature decreases monotonically with increasing B concentration suggests that the increasing B concentration lead to decrease Co−Co interactions. Both the decrease of exchange interaction and magnetic dilution result in a rapid decrease of T_C with increasing B concentration.

The field dependence of magnetization for the free powder samples of $Nd_{m+n}Co_{5m+3n}B_{2n}$ was measured at 5 K in a SQUID in a magnetic field ranging from 0 to 65 kOe. These powder particles are nearly single crystal ($\leq 40\ \mu$m) and small enough to orient themselves in the external field. The saturation moment was derived by fitting the experimental data of $M(H)$ versus H using the law of approach to saturation. The intrinsic magnetic parameters of $Nd_{m+n}Co_{5m+3n}B_{2n}$ are given in Table 4, including Curie temperature (T_C), spin−reorientation temperature (T_{SR}), saturation magnetization (M_S) at 5 K, average Co moment ($\langle\mu_{Co}\rangle$), anisotropy fields (H_A) at 5 K, and the EMD at room temperature. The coupling of the magnetic moments in the ternary $Nd_{m+n}Co_{5m+3n}B_{2n}$ borides is similar to that observed in binary R−T intermetallics, i.e., there is antiferromagnetic coupling between Co spins and the R spins. For $Nd_{m+n}Co_{5m+3n}B_{2n}$ in which Nd is a light R element ($\mathbf{J} = \mathbf{L} - \mathbf{S}$) this implies that the total R moment ($g\mathbf{J}\mu_B$) is coupled parallel to the Co moments. Therefore, the magnetic moments of $Nd_{m+n}Co_{5m+3n}B_{2n}$, μ_s, can be expressed as

$$\mu_s = (m + n)\langle\mu_{Nd}\rangle + (5m+3n)\langle\mu_{Co}\rangle \qquad (4)$$

$\langle\mu_{Nd}\rangle$ and $\langle\mu_{Co}\rangle$ are the average moment of Nd atoms and Co atoms, respectively. Reliable values of the saturation moment of Co may be obtained for Gd (s-state) or Y (nonmagnetic) compounds. In compounds with non-s-state R ions, the Co moment in general cannot be accurately determined because of the unknown reduction of the R moment by crystal field effects or because of difficulties in saturating the compounds as a result of their high anisotropy. However, it is possible to estimate the moment of the Co sublattice in these systems, if information is available about the R moment. If we assume the average Nd^{3+} moment to be 3 μ_B, $\langle\mu_{Co}\rangle$ of $Nd_{m+n}Co_{5m+3n}B_{2n}$ are calculated and the results are shown in Figure 5b

Table 5. Magnetic Moment of the Co(N) in $Nd_{m+n}Co_{5m+3n}B_{2n}$ Borides, Where Co(N) Means a Co Atom Which Has NB Layers Just Above or Just Below

	$\mu_{Co(0)}$ (μ_B)	$\mu_{Co(1)}$ (μ_B)	$\mu_{Co(2)}$ (μ_B)
(1) $NdCo_5$	1.2		
(2) $Nd_3Co_{13}B_2$	1.2	0.6	
(3) $NdCo_4B$	1.2	0.5	
(4) $Nd_5Co_{19}B_6$	1.2	0.2	0
(5) $Nd_3Co_{11}B_4$	1.2	0.1	0
(6) $Nd_2Co_7B_3$	1.2	0	0

It is reasonable to assume that the Co atoms at different crystallographic sites have different magnetic moment. As seen in Figure 2a−g, the different Co crystallographic sites can be expressed by Co(N) with $N = 0$, 1, and 2, where Co(N) means a Co atom which has NB layers just above or just below. In $Nd_3Co_{13}B_2$, there are six Co(1) and seven Co(0) atoms, thus the average Co moment of $Nd_3Co_{13}B_2$ is expressed by

$$\langle\mu_{Co}\rangle = [4\langle\mu_{Co(0)}\rangle + 3\langle\mu_{Co(0)}\rangle + 6\langle\mu_{Co(1)}\rangle]/13 \qquad (5)$$

In $Nd_5Co_{19}B_6$, there are three Co(2), twelve Co(1), and four Co(0) atoms, thus the average Co moment of $Nd_5Co_{19}B_6$ is expressed by

$$\langle\mu_{Co}\rangle = [4\langle\mu_{Co(0)}\rangle + 6\langle\mu_{Co(1)}\rangle + 6\langle\mu_{Co(1)}\rangle + 3\langle\mu_{Co(2)}\rangle]/19 \qquad (6)$$

Similarly, the average Co moment of $Nd_{1+n}Co_{5+3n}B_{2n}$ is expressed by

$$\langle\mu_{Co}\rangle = [2\langle\mu_{Co(0)}\rangle + 6\langle\mu_{Co(1)}\rangle + 3(n-1)\langle\mu_{Co(2)}\rangle]/(3n+5) \qquad (7)$$

where $\mu_{Co(N)}$ means the magnetic moment of the Co(N). The Co(2) atom has B layers just above and below and the B valence electrons may be expected to fill the Co-(2)-3d bands. Therefore, we assume that $\langle\mu_{Co(2)}\rangle$ is zero, as is found in RCo_3B_2 compounds.[30] The nearest-neighbor environment of Co(0) at the $4h_1$ position is unchanged with respect to the corresponding site in $NdCo_5$, so that $\mu_{Co(0)}$ may be assumed to keep the value of 1.2 μ_B.[31] By inserting the above values for $\mu_{Co(0)}$ and $\mu_{Co(2)}$ and the observed value for $\langle\mu_{Co}\rangle$ of $Nd_3Co_{13}B_2$ into eq 2, a value of 0.6 μ_B is obtained for $\mu_{Co(1)}$. So, $\mu_{Co(0)}$, $\mu_{Co(1)}$, and $\mu_{Co(2)}$ are 1.2, 0.6, and 0 μ_B, respectively. The values of $\langle\mu_{Co(N)}\rangle$ for other borides in this series are also calculated and the results are presented in Table 5, showing that the introduction of B results in a strong decrease of the Co moment. Band−structure calculations[32] have shown that the p−d hybridization lowers

(30) Ido, H.; Nanjo, M.; Yamada, H. *J. Appl. Phys.* **1994**, *75*, 7140.
(31) Ito, T.; Asano, H.; Ido, H.; Yamada, M. *J. Appl. Phys.* **1996**, *79* (8), 5507.
(32) Aoki, M.; Yamada, H. *Physica B* **1992**, *177*, 259.

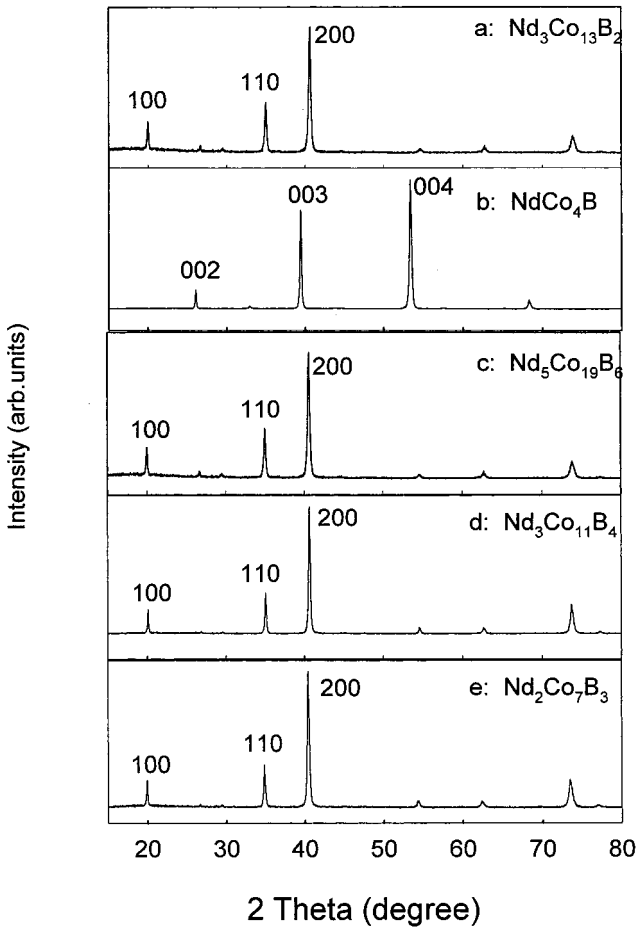

Figure 6. The XRD patterns of the magnetically aligned $Nd_{m+n}Co_{5m+3n}B_{2n}$ compounds.

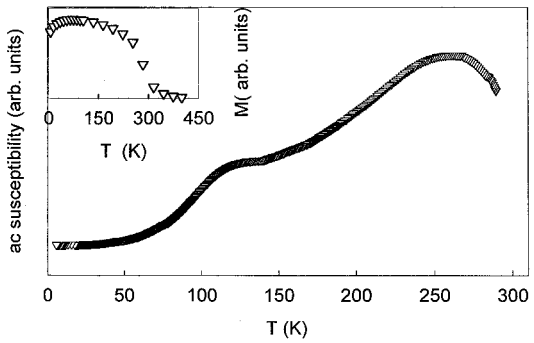

Figure 7. Temperature dependence of the real component (χ') of the ac susceptibility of bulk $Nd_3Co_{11}B_4$ sample. Inset shows the $M(T)$ curve of $Nd_3Co_{11}B_4$.

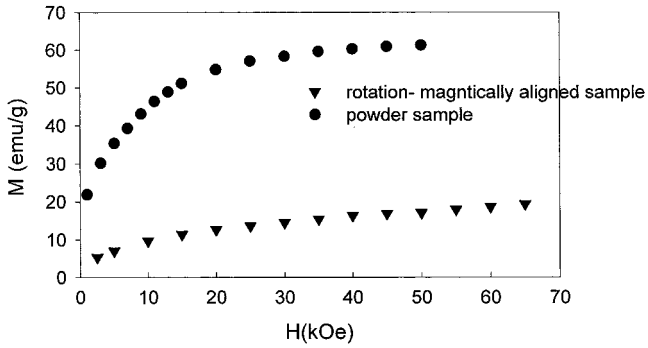

Figure 8. Field dependence of the magnetization measured in a SQUID at 5 K for free powder $Nd_3Co_{11}B_4$ (filled cycles) and the rotation-aligned $Nd_3Co_{11}B_4$ (filled triangles) with the applied field parallel to the hard magnetization direction.

the density of states at Fermi energy and reduces the 3d band splitting when B atoms preferentially substitute into the nearest-neighbor sites of the Nd atoms.

Figure 6 illustrates the room temperature XRD patterns of magnetically aligned samples of $Nd_{m+n}Co_{5m+3n}B_{2n}$. It can be seen that the patterns of oriented $Nd_3Co_{13}B_2$, $Nd_5Co_{19}B_6$, $Nd_3Co_{11}B_4$, and $Nd_2Co_7B_3$ samples contain the peaks of (100), (200), and (110). The results clearly demonstrate that the EMD of these borides lie in the basal plane at room temperature. An anomaly was observed at around 370 K in the $M(T)$ curves of $Nd_3Co_{13}B_2$ and this corresponds to spin−reorientation transition. In our previous paper,[25] the measurement of the temperature dependence of the magnetization was only performed in the range from 298 to 500 K, and we mistook the T_{SR} as T_C. After we carefully studied the $Nd_3Co_{13-x}Ni_xB_2$ system, we have deduce that $Nd_3Co_{13}B_2$ has T_C of 710 K and exhibits uniaxial anisotropy above the T_{SR} and planar anisotropy below T_{SR}.

The $M(T)$ and as susceptibility χ' vs T curves of the bulk $Nd_3Co_{11}B_4$ sample are illustrated in Figure 4d and Figure 7, respectively. The value of the as susceptibility χ' of an intermetallic compound depends strongly on its magnetic anisotropy and domain-wall energy. It is proportional to $M_S^2/(AK_1)^{1/2}$ for domain-wall displacement or M_S^2/K_1 for domain rotation. Both saturation magnetization M_S and anisotropy constant K_1 strongly vary with temperature; thus the shape of the χ' vs T curve is strongly affected by the temperature dependence of M_S and K_1. At the spin−reorientation temperature, the change of M_S is relatively smooth, while K_1 changes drastically, which is reflected as a kink in the χ' vs T curves. The spin−reorientation temperature T_{SR} can be taken as the temperatures at which the first deviative of the as susceptibility $d\chi'/dT$ reaches an extreme value (maximum or minimum). Measurements of temperature dependence of the ac susceptibility can be therefore used to detect temperature-induced magnetic-phase transitions. The broad peak in the χ' vs T curve (Figure 7) at the temperature of 275 K correspond to its Curie temperature. An anomaly is visible at around 100 K. Considering the temperature-induced competition between the planar Nd sublattice anisotropy and the uniaxial Co sublattice anisotropy, as mentioned below, one can attribute this anomaly to spin−reorientation. Figure 8 shows the magnetic isothermal measured in a SQUID at 5 K of free powder $Nd_3Co_{11}B_4$ (filled cycles) and the rotation-aligned sample (filled triangles) with the applied field parallel to the HMD. This result suggests that the EMD of $Nd_3Co_{11}B_4$ only change from easy-plane at room temperature to easy-cone at low temperature. Otherwise, if the EMD of $Nd_3Co_{11}B_4$ changes from easy-plane to easy-axial, the field dependence should be the same for the magnetization of the free powder $Nd_3Co_{11}B_4$ (filled cycles) and the HMD of rotation-aligned sample (filled triangles).

It can be seen in Figure 6b that the room-temperature XRD pattern of oriented sample of $NdCo_4B$ contains the peaks of (002), (003), and (004). Thus, the EMD of $NdCo_4B$ is parallel to the c axis at room temperature and does not change from 5 K to its Curie temperature, as evidenced in its $M(T)$ curve (Figure 4b). This can most easily be explained that the Co sublattice uniaxial

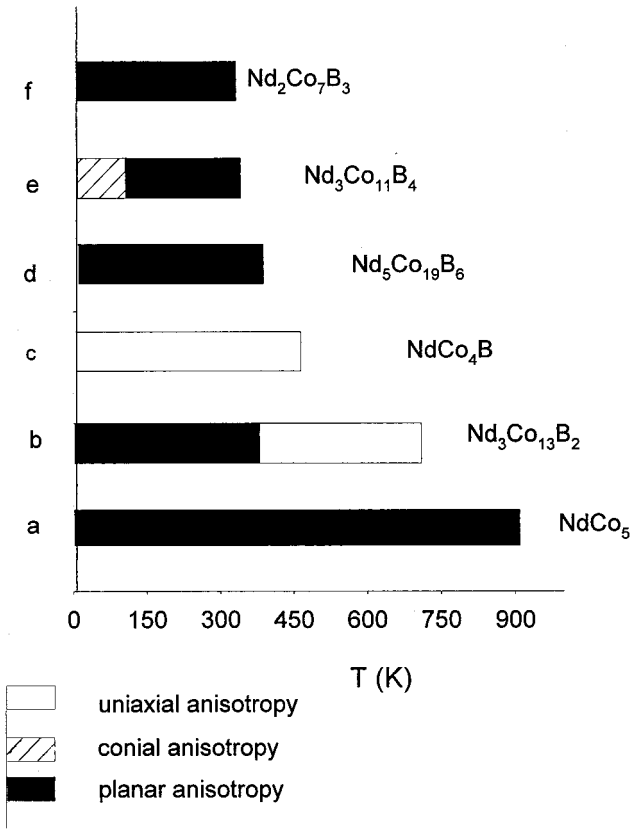

Figure 9. Magnetic phase diagram of the $Nd_{m+n}Co_{5m+3n}B_{2n}$ borides.

anisotropy always overcomes the Nd sublattice planar anisotropy. While $Nd_5Co_{19}B_6$ and $Nd_2Co_7B_3$ have plane anisotropy from 5 K to their Curie temperatures. Finally, the magnetic phase diagram of the $Nd_{m+n}Co_{5m+3n}B_{2n}$ compounds is illustrated in Figure 9. To measure the magnetocrystalline anisotropy of these borides, the field dependence of magnetization of the magnetically aligned samples were measured in a SQUID. By linearly extrapolating ΔM to zero on the ΔM $(= M_{\parallel} - M_{\perp}) - H$ curve, the anisotropy field H_A are derived and shown in Table 4, showing that the increasing B results in a enhancement of the magnetocrystalline anisotropy. Previous ^{155}Gd Mössbauer studies[27] of the series $GdCo_4B$, $Gd_3Co_{11}B_4$, $Gd_2Co_7B_3$, and $GdCo_3B_2$, show that the second-order crystal-electric field (CEF) coefficient A_{20} increases with increasing B substitution. Averaged over the R sites, A_{20} reaches -700, -1000, -1200, -1600, -2200 Ka_0^{-2} in RCo_5, RCo_4B, $R_3Co_{11}B_4$, $R_2Co_7B_3$, and RCo_3B_2, respectively, Generally, the second-order CEF coefficient A_{20} is fairly constant in a series of isostructual R compounds in which only the R component is varied. It seems reasonable, therefore, to use the A_{20} values obtained from the $Gd_{m+n}Co_{5m+3n}B_{2n}$ compounds for analyzing CEF effects in the corresponding Nd compounds. This can explain the increase in magnetocrystalline anisotropy of $NdCo_{5-x}B_x$ with increasing B concentration.

It is well-known that the net anisotropy in rare earth-Co compounds is determined by the sum of the rare earth sublattice anisotropy and the Co sublattice anisotropy. In the case of $R_{m+n}Co_{5m+3n}B_{2n}$ compounds

$$K_{1,\mathrm{tot}} = (m+n)K_{1,\mathrm{R}} + K_{1,\mathrm{Co}} \quad (8)$$

where $K_{1,R}$ is the contribution of one R^{3+} ion to the anisotropy constant and $K_{1,Co}$ is the anisotropy constant of the Co sublattice. In first approximation, $K_{1,R}$ can be described as

$$K_{1,\mathrm{R}} = -3/2\alpha_J A_{20}\langle r^2_{4f}\rangle\langle 3J^2_{\mathrm{R},z} - J_{\mathrm{R}}(J_{\mathrm{R}}+1)\rangle \quad (9)$$

where α_J is the second-order Stevens coefficient. The occurrence of a spin−reorientation in $Nd_3Co_{13}B_2$ with increasing temperature can be understood as follows: The contribution of Nd sublattice to magnetocrystalline anisotropy, which plays a more important role in determining the EMD at low temperatures, arises from the coupling between Nd ion orbit magnetic moment and the crystal electric field. It is dependent on the product of α_J and A_{20}. A negative $\alpha_J A_{20}$ exhibits a uniaxial anisotropy.[2] As mentioned above, A_{20} is negative in the $R_{m+n}Co_{5m+3n}B_{2n}$ compound.[33] The rare earth Nd has a negative α_J: accordingly, $Nd_3Co_{13}B_2$ has an easy planar anisotropy at low temperature. As the temperature increases, the crystal-field-induced Nd sublattice anisotropy becomes in less important due to the strong temperature dependence of the $O^0_2 = \langle 3J_z^2 - J(J+1)\rangle$ term. This means that when increasing the temperature, the easy-axis Co lattice anisotropy in $Nd_3Co_{13}B_2$ has to compete with the Nd sublattice anisotropy, giving rise to a preferred moment direction parallel to the *c* axis. The spin reorientation temperature marks the point at which both sublattices have equal contribution.

As the nonmagnetic B concentration increases in this homologous series $NdCo_{5-x}B_x$, more and more B atoms substitute for Co atoms at the sites related to the 2c site of RCo_5 structure, which primarily responsible for the large positive anisotropy contribution. The temperature-induced competition between the planar Nd sublattice anisotropy and the uniaxial Co sublattice anisotropy lead to a complex magnetic phase diagram in this system.

Curie temperature, saturation magnetic moment and magnetocrystalline anisotropy are the fundamental intrinsic magnetic parameters of permanent magnets. High Curie temperature can guarantee the magnets to have low-temperature coefficients of the hard magnetic properties so that they can be applied over a wide temperature range. Large values of the uniaxial magnetocrystalline anisotropy are required to achieve high coercivities. To further improve the magnetic properties of these Nd−Co−B borides, the most effective way is to synthesize new Co-rich phases with *combined structures*, which is formed by stacking of different crystal structures. Here we list some promising combinations of different structures and some of the compositions generated by these formulas can be regarded as real compound compositions:

$$m\mathrm{RCo_5} + n\mathrm{RCo_3B_2} = \mathrm{R_{m+n}Co_{5m+3n}B_{2n}} \quad (10)$$

$$m\mathrm{R_2(CoM)_{17}} + n\mathrm{RCo_3B_2} = \mathrm{R_{2m+n}(CoM)_{17m+3n}B_{2n}} \quad (11)$$

$$m\mathrm{R(CoM)_{12}} + n\mathrm{RCo_3B_2} = \mathrm{R_{m+n}(Co\,M)_{12m+3n}B_{2n}} \quad (12)$$

(33) Huang, M. Q.; Ma, B. M.; Cheng, S. F.; Wallace, W. E. *J. Appl. Phys.* **1991**, *69*, 55.

The expansion of binary R−T alloys to ternary alloys including metalloids, especially boron, is an important development in permanent materials. It is high time to exploit the these quaternary phases in the Co-rich side of the R−Co−M−B systems. The Sm compounds, where the rare earth and coblat contributions are not in competition, but both favor the axis, are the particular interesting and are themselves worthy of further study. Such a systematic investigation is underway in our laboratory.

Acknowledgment. This work was supported by International Center for Diffraction Data (ICDD) Crystallography Scholarship Award, the National Natural Science Foundation of China, and the State Key Project for Fundamental Research in China. The authors also express their gratitude to X. R. Cheng and T. S. Ning for their assistance in the X-ray diffraction experiments.

CM990462F